Sensors & Transducers, Vol. 191, Issue 8, August 2015, pp. 57-62

www.sensorsportal.com

Sensors & Transducers

http://www.sensorsportal.com

CeB_6 Sensor for Thermoelectric Single-Photon Detector

*** Armen KUZANIAN, Vahan NIKOGHOSYAN, Astghik KUZANYAN**
Material Science Lab., Institute for Physical Research, Ashtarak-2, 0203, Republic of Armenia
* Tel.: +374 10288150, fax: +374 23231172
* E-mail: akuzanyan@yahoo.com

Received: 24 June 2015 /Accepted: 30 July 2015 /Published: 31 August 2015

Abstract: Interest in single-photon detectors has recently sharply increased. The most developed single-photon detectors are currently based on superconductors. Following the theory, thermoelectric single-photon detectors can compete with superconducting detectors. The operational principle of thermoelectric detector is based on photon absorption by absorber as a result of which a temperature gradient is generated across the sensor. In this work we present the results of computer modeling of heat distribution processes after absorption of a photon of 1 keV - 1 eV energy in different areas of the absorber for different geometries of tungsten absorber and cerium hexaboride sensor. The time dependence of the temperature difference between the ends of the thermoelectric sensor and electric potential appearing across the sensor are calculated. The results of calculations show that it is realistic to detect single photons from IR to X-ray and determine their energy. Count rates up to hundreds gigahertz can be achieved. *Copyright © 2015 IFSA Publishing, S. L.*

Keywords: Sensor, Absorber, Thermoelectric, Single-photon detector, Photon energy, Count rate.

1. Introduction

Intensive development of science and engineering requires new generations of devices for precise measurements. Interest in single-photon detectors (SPDs) has recently increased dramatically, due to many novel applications in various research fields, such as quantum communication, quantum cryptography, space astronomy, chemical analysis, particle physics, medical applications, traditional and quantum-enabled metrology and others [1]. The most developed SPDs are currently based on superconductors [2]. Over the last fifteen years superconducting nanowire single-photon detectors (SNSPD) are actively investigated because of their high system detection efficiency, low dark count rate, high counting rate and timing resolution [3]. Following the theory, thermoelectric detectors (TSPD) can compete with superconducting detectors [4] and thermoelectric nanowire single-photon detector (TNSPD) with superconducting nanowire single-photon detectors [5].

Sensitivity of thermoelectric devices to single photons is determined by the signal/noise ratio, the consideration of which gives acceptable energy resolution. Thus, to provide the energy resolution of 1 eV at a single-photon absorption, the thermoelectric material must have a Seebeck coefficient of ~ 100 μV/K. Materials with a higher Seebeck coefficient are abundant, but the point is that in order to achieve the required signal/noise ratio, the detector must operate at very low temperatures. One of the well-known low temperature thermoelectric materials is the gold with iron impurities. However, in our opinion, cerium hexaboride (CeB_6) is more promising [6-7].

2. Methodology

2.1. Thermoelectric Single-photon Detector

The operational principle of TSPD is based on photon absorption by absorber as a result of which a temperature gradient is generated across the sensor. Photon detection becomes possible by measuring the potential, emerging between the two absorbers. The scheme of the TSPD sensitive element is given on Fig. 1. Such a sensor does not require either a separate power unit or a bias voltage. Therefore, it does not need additional leads for electronic circuitry either, and a matrix detector built on them will have a very simple engineering and electronic structure. Materials which can be used to prepare the absorber and the sensor and the achievable count rates and energy resolution are given in publications [4-6]. A conclusion is done according which the thermoelectric detector may possess an energy resolution of 0.1 eV and a gigahertz level count rate.

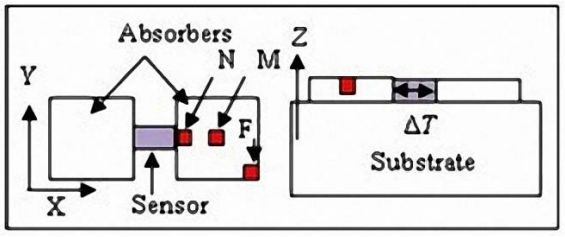

Fig. 1. The detection pixel of TSPD.

In this work we present the results of computer modeling of the TNSPD. We observe the processes of heat distribution after absorption of a photon of 1 eV (IR), 10 eV (UV), 100 eV (hard UV) and 1 keV (X-rays) energy in different areas of the absorber (points N, M and F in Fig. 1) for different geometries of tungsten absorbers and CeB_6 sensor. Fig. 1 also shows the directions of coordinate axes: *x* is parallel to the axis of symmetry of the sensor (corresponding to the length of geometric shapes), *y* is perpendicular to *x* (width), *z* is perpendicular to *x, y* and to the substrate surface (height).

2.2. Computing Technique

The calculations were based on the heat conduction equation. For simplicity of calculations in a first approximation, the phonon contribution to the heat capacity is not taken into account. The time dependence of the temperature difference between the ends of the thermoelectric bridge (ΔT) and electric potential (ΔU) appearing across the sensor are calculated. The calculations were carried out by the matrix method for differential equations [7]. The operating temperature of the detector was taken to be 9 K. The materials used have the parameters presented in Table 1 [8-11].

Table 1. Parameters of used materials at 9 K.

Parameters	Unit	W	CeB_6
Density, ρ	kg/m^3	19250	4800
Specific heat capacity, *c*	J/kg·K	0.0026	0.196
Electronic contribution to specific heat capacity, *γ*	J /kg·K^2	0.022	0.813
Thermal conductivity, *λ*	W/m·K	9680	0.94
Seebeck coefficient, *S*	μV/K	-	150

The modeling of thermal processes occurring in the absorption of a photon is as follows. The entire volume of the absorber and the bridge was broken down into a cell of the size Δx, Δy and Δz. These dimensions were typically of the order of 0.1 μm. Obviously, the greater the number of cells will provide the more accurate the calculation, but more time consuming.

The thermal processes were modeled according to the following algorithm.

- For all cells the initial temperature was set to 9 K. The cell where the photon is absorbed was chosen in the absorber.
- According to the formula $\Delta T = E/V\rho c$, where E is the energy of the absorbed photon and V is the cell volume, the initial temperature of the cell $T_0 = 9\ \text{K} + \Delta T$ was calculated.
- The temperature of all the cells for each time point t_n was determined.
- As can be seen in Fig. 1, the sensor is composed of two absorbers of the same size.

As shown in [12], photons with an energy of 1 keV are absorbed with a ~ 100 % probability in a 1.5 μm thick tungsten, photons with an energy of 100 eV - in a 0.5 μm thick tungsten. We can also calculate that photons with 10 eV and 1 eV energy are almost completely absorbed in the tungsten absorber with a thickness of 0.1 μm. And this thickness values for absorbers and the thermoelectric sensor is used in calculations.

One of the main characteristics of thermoelectric sensors is the time of the heat flow through the metal–insulator boundary (τ_K), which is called the Kapitza boundary [4]. This time is calculated by the formula

$$\tau_K = r_0 * C_{abc} / T^3 * A_{abc}, \quad (1)$$

where A_{abs} is the contact surface area, and at low temperatures $r_0 \sim 20\ \text{K}^4\ \text{cm}^2/\text{W}$. If we substitute in this equation the heat capacity of tungsten at the temperature of 9 K (Table 1), we obtain the corresponding values of τ_K = 1.04, 5.2, 15.6, 31.2 and 52 ps for the absorber thickness value of 0.1, 0.5, 1.5, 3, and 5 μm, respectively. These are times that limit the transfer of heat of an absorbed photon from one absorber to another absorber through the thermoelectric bridge. Only for these time intervals a voltage will arise between the absorbers, by measuring which we can register the fact of photon absorption. We will try to find out below how

feasible it is and what voltage may arise between the absorbers during the absorption photons with 1 keV - 1 eV energy.

3. Results

3.1. Registration of Photons with Energy of 100 eV

The equation of heat distribution from a limited volume in a three-dimensional model was solved for various geometries of the thermoelectric sensor with boundary conditions of absence of heat transfer to the medium and a slight loss of the heat to the substrate. Table 2 shows the calculation numbers (capital letters correspond to the absorber areas with impingent photons), data on the absorber and the sensor size (x, y, z), photon energy E, maximum temperature difference ΔT_{max} at the ends of the bridge, the time $t(\Delta T_{max})$ in which this maximum is reached, the voltage ΔU_{max} (calculated using the Seebeck coefficient value $S = 150$ μV/K at 9 K), the time of the gradient fall to the background values $t(\Delta T_{max}/10)$ and the detector count rate $R = 1/t(\Delta T_{max}/10)$.

Data of Table 2 will be discussed in parallel with the consideration of the time dependence of the temperature difference at the ends of the thermoelectric bridge $\Delta T(t)$. In Fig. 2 and Fig. 3, these dependences are given for the absorbers with the dimensions of 10×10×0.5 μm^3 and 10×0.5×0.5 μm^3 respectively. The insets show the numbers of calculations and the size of the bridge.

Table 2. Sensor geometry, ΔT_{max}, ΔU_{max} and count rate (R) for E=100 eV photon.

No.	W absorber size, (μm)	CeB6 sensor size, (μm)	E, (eV)	ΔT_{max}, (10^{-4} K)	ΔU_{max}, (nV)	$t(\Delta T_{max})$, (ps)	$t(\Delta T_{max}/10)$, (ps)	R, (GHz)
1M	10×10×0.5	1×1×0.5	100	0.842	12.6	104.1	>5000	<0.2
2M	10×10×0.5	0.1×1×0.5	100	0.839	12.58	75.6	>5000	<0.2
3M	10×10×0.5	0.01×1×0.5	100	0.697	10.5	15	>5000	<0.2
4M	10×10×0.5	0.01×5×0.5	100	0.602	9	13.8	422	**2.4**
5M	10×10×0.5	0.01×10×0.5	100	0.47	7	13.2	242	**4.2**
6M	10×10×0.5	0.1×10×0.5	100	0.828	12.4	32.4	>2000	<0.5
7M	10×0.5×0.5	0.01×0.5×0.5	100	8.79	131.9	11.7	254	**3.9**
8M	10×0.5×0.5	0.1×0.5×0.5	100	15.6	234	32.4	>2000	<0.5
9M	10×0.5×0.5	1×0.5×0.5	100	15.9	238	39	>2000	<0.5
10M	5×0.5×0.5	0.1×0.5×0.5	100	31.3	469	15	>5000	<0.2
11N	5×0.5×0.5	0.1×0.5×0.5	100	136	2040	0.3	>2000	<0.5
12F	5×0.5×0.5	0.1×0.5×0.5	100	31.2	468	21.6	>5000	<0.2
13M	5×0.5×0.5	0.1×0.5×0.5	**110**	34.4	516	14.1	>5000	<0.2
14M	5×0.5×0.5	0.1×0.5×0.5	**90**	28.1	421.5	12.3	>5000	<0.2

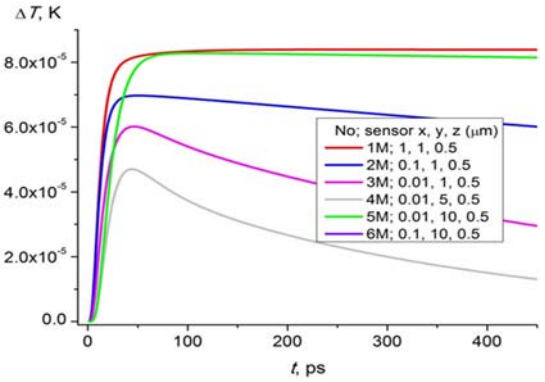

Fig. 2. $\Delta T(t)$ dependence for case of W absorber with the size of 10×10×0.5 μm^3, photon E = 100 eV.

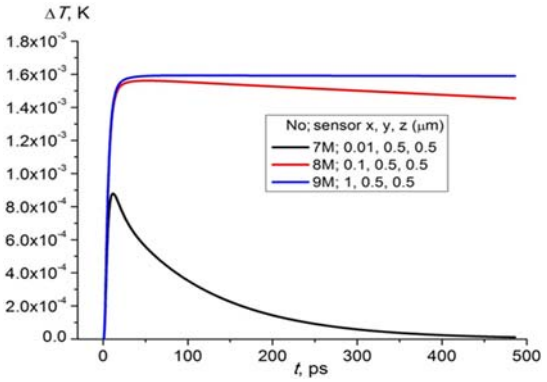

Fig. 3. $T(t)$ dependence for a case of W absorber with the size of 10×0.5×0.5 μm^3, photon E = 100 eV.

As can be seen in Fig. 2, for the bridge length of 1, 0.1 μm and a width of 1 μm (1M, 2M) the decline of ΔT after reaching a maximum is very slow. If we extend the bridge to the width of the absorber 10 μm (6M), it decreases the ΔTmax value and the decline in ΔT is faster. However, a decrease in the length of the bridge to 0.01 μm (3 M – 5 M) has a more significant impact on the variation of these parameters.

The most encouraging is the curve corresponding to the calculation 5M. At the same time, according to both Table 2 and Fig. 2 data, for the absorber size of 10×10×0.5 μm^3 values ΔT less than 10^{-4} K are achieved. Reducing the volume of the absorber 20 times leads to a significant increase in the achievable ΔT_{max} values. Fig. 3 shows plots of ΔT(t) for three values of the bridge length – 1, 0.1 and 0.01 μm. And once again we see that the decrease in the length of the bridge leads, as might be expected, to some reduction of ΔT_{max} and acceleration in the decline of ΔT after the maximum.

Let us further reduce the volume of the absorber two times and consider the influence on the $\Delta T(t)$ of the location of the photon thermalization zone (Fig. 1) and of changes in the photon energy by 10 %. Fig. 4 and Fig. 5 show the results of these calculations for the bridge lengths of 0.1 (Table 2) and 0.01 μm (Table 3) respectively.

We first note the similarity of calculations presented in Fig. 4 and Fig. 5.

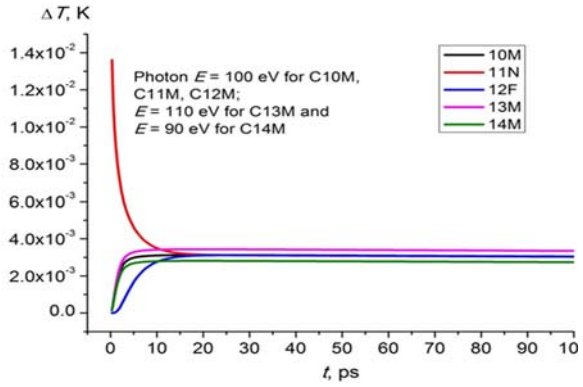

Fig. 4. $\Delta T(t)$ dependence for a case of W absorber with the size of 5×0.5×0.5 μm^3, CeB_6 sensor - 0.1×0.5×0.5 μm^3.

Significantly differ the $\Delta T(t)$ curves for the calculations labeled M, N and F. At the length of the bridge of 0.1 μm this difference is leveled for t > 20 ps, whereas for the bridge length of 0.01 μm the difference holds longer. If the photon energy is different by 10 eV (calculations 10M, 13M and 14M), the ΔT_{max} differs by ~ 3.2×10^{-4} K. With the value of the Seebeck coefficient of 150 μV/K, this provides the build-up of a ~ 50 nV voltage – a quantity that can be detected without the use of special electronics, distinguishing photons with energy of 100 ± 10 eV.

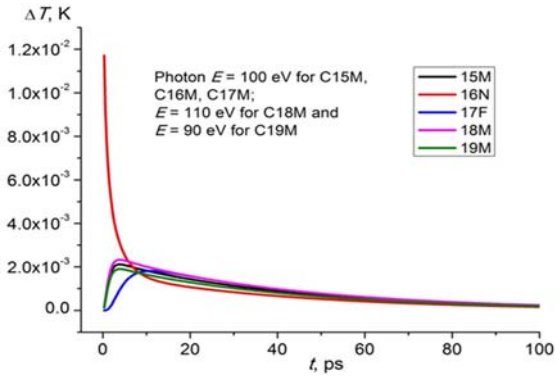

Fig. 5. $T(t)$ dependence for case of W absorber with the size of 5×0.5×0.5 μm^3, CeB_6 sensor - 0.01×0.5×0.5 μm^3.

Table 3. Sensor geometry, ΔT_{max}, ΔU_{max}, $t(\Delta T_{max}/10)$, and count rate R for E=1 eV – 1 keV photon.

No.	W absorber size, (μm)	CeB_6 sensor size, (μm)	E, (eV)	ΔT_{max}, (10^{-4} K)	ΔU_{max}, (nV)	$t(\Delta T_{max})$, (ps)	$t(\Delta T_{max}/10)$, (ps)	R, (GHz)
15M	5×0.5×0.5	0.01×0.5×0.5	100	21.1	316.5	3.6	101.1	9.89
15Ma	5×0.5×0.5	0.01×0.5×0.5	10	2.11	31.65	3.9	101.1	9.89
15Mb	5×0.5×0.1	0.01×0.5×0.1	10	11	165	3.12	100	10
15c	5×0.5×0.5	0.01×0.5×0.5	1	0.211	3.165	3.9	101.1	9.89
15d	5×0.5×0.1	0.01×0.5×0.1	1	1.07	16	3.81	101.43	9.86
16N	5×0.5×0.5	0.01×0.5×0.5	100	337	5055	0.033	3.5	286
16Na	5×0.5×0.5	0.01×0.5×0.5	10	34	510	0.03	3.38	**286**
16Nb	5×0.5×0.1	0.01×0.5×0.1	10	78	1170	0.096	9.819	**101.8**
16Nc	5×0.5×0.5	0.01×0.5×0.5	1	3.37	50	0.033	3.42	**292.4**
16Nd	5×0.5×0.1	0.01×0.5×0.1	1	7.8	117	0.114	9.819	**101.8**
17F	5×0.5×0.5	0.01×0.5×0.5	100	18.1	271.5	10.2	111.6	8.96
17Fa	5×0.5×0.5	0.01×0.5×0.5	10	1.81	27	10.8	111.6	8.96
17Fb	5×0.5×0.1	0.01×0.5×0.1	10	9.1	137	10.92	112.2	8.9
17Fc	5×0.5×0.5	0.01×0.5×0.5	1	0.181	2.7	10.8	111.6	8.96
17Fd	5×0.5×0.1	0.01×0.5×0.1	1	0.91	13.7	10.92	112.2	8.9
18M	5×0.5×0.5	0.01×0.5×0.5	**110**	23.2	348	3.6	101.1	9.89
19M	5×0.5×0.5	0.01×0.5×0.5	**90**	19	285	3.6	101.1	9.89
23M	5×5×1.5	0.01×5×1.5	1000	8.54	130	2.1	51.3	19.5
26N	5×5×1.5	0.01×5×1.5	1000	19.8	230	0.6	26.7	37.5
27F	5×5×1.5	0.01×5×1.5	1000	8.7	130	3.9	52.8	18.9
28M	5×5×1.5	0.01×5×1.5	**1100**	9.36	140	2.1	51	19.6
29M	5×5×1.5	0.01×5×1.5	**900**	7.68	120	2.1	49.7	20.1

3.2. Registration of Photons with an Energy of 1 eV, 10 eV and 1 keV

In Fig. 6 $\Delta T(t)$ dependences are given for the absorbers with dimensions 5×5×1.5 μm^3 for absorption of photon with an energy of 1 keV. The $\Delta T(t)$ curves significantly differ for calculations labeled M, N and F. From comparison of curves 23M and 27F it is seen that photon absorption in a region far from the thermoelectric bridge of the absorber,

relative to photon absorption in the center, leads to a slight increase of ΔT_{max} and increase of $t(\Delta T_{max})$. Let us note that calculations of 23M and 27F were done for similar values of the absorber and bridge dimensions. Calculation 26N were also done for similar dimensions of the absorber and of the bridge; the letter N corresponds to photon absorption in vicinity of the thermoelectric bridge. In this case the time dependence of ΔT has a different profile. As it can be seen from Fig. 6, the curve 26N attains significantly higher values of ΔT in a shorter time interval. The difference between 23M and 26N disappears at t >50 ps.

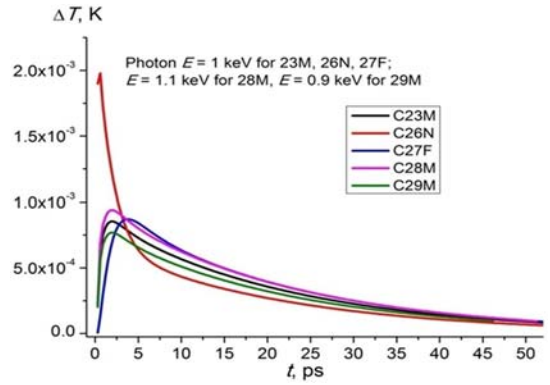

Fig. 6. $T(t)$ dependence for case of W absorber with the size of 5×5×1.5 μm^3, CeB_6 sensor - 0.01×5×1.5 μm^3.

If the photon energy differs by 100 eV, the ΔT_{max} differs by 7.7 mK (28M, 29M - Table 3). With the value of the Seebeck coefficient of 150 μV/K for CeB_6 at 9 K, this provides the build-up of a ~ 10 nV voltage. If we can measure with a high confidence the voltage of 1 nV, then we can be similarly confident in distinguishing photons of 1000±10 eV energies.

The calculation results of 15Ma-15Md are presented in Fig. 7. From comparison of 15Ma, 15Mc (z=0.5 μm) and 15Mb, 15Md (z=0.1μm) curves it is seen that photon absorption in detection pixel with a smaller thickness leads to the significant increase of ΔT value. As can be judged from the data of Table 3, even in the absorption of 1 eV photons, the value of the voltage more than 10 nV is obtained. We can say that a photon with this energy can be registered and its energy can be determined.

Let's compare the values of the time in which ΔT_{max} is reached (presented in Table 2 and Table 3) with the values of the time of the heat flow through the Kapitza boundary (τ_K), given in Section 2.2. The values of $t(\Delta T_{max})$ calculations in Table 2 are greater than τ_K = 5.2 ps (for the absorber thickness 0.5 μm). It means that the maximum value ΔT_{max} for the geometries of absorber and sensor discussed in this table will not be achieved. The heat will move to the dielectric substrate. An exception is the calculation for the case when a photon is absorbed in immediate proximity from the sensor (11N), but it is a particular case the possibility of which is small. Thus, we can say that such detector can detect a single photon absorption fact, but maximum values of ΔT_{max} and ΔU_{max} will not be achieved.

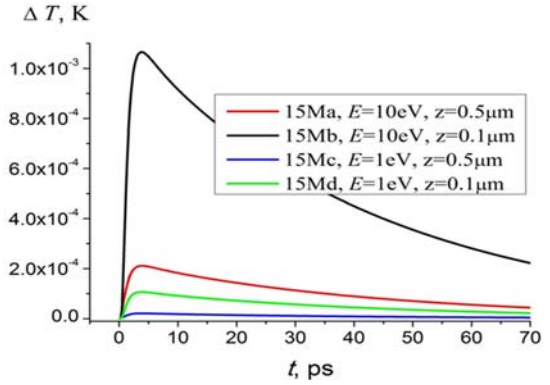

Fig. 7. $\Delta T(t)$ dependence for 10 eV and 1 eV photon absorption in case of different thickness (z) of detection pixel.

The situation is completely different for the calculations presented in Table 3. For all the calculations corresponding to the thicknesses of the absorber 0.5 μm and 1.5 μm the values of $t(\Delta T_{max})$ are less than values of τ_K=5.2 ps and τ_K=15.6 ps, respectively. In Table 3 only calculations marked 17F don't correspond to this rule. Comparison of values of the parameters $t(\Delta T_{max}/10)$ and τ_K shows that in some cases the counting rate will be determined by the first, in other cases – by the second parameter. For those sizes of absorber and sensor for which $\tau_K < t(\Delta T_{max}/10)$, the counting rate will be equal to ~ 180 GHz for the thickness of the absorber 0.5 μm, and about 60 GHz for the thickness of 1.5 μm.

4. Conclusions

According to the results of calculations can be stated that detection of single photons from IR to X-ray and the possibility to define their energy by accuracy no less than 10 % is realistic. It is possible without additional amplification of the obtained signals for their registration while providing count rates exceeding 100 GHz!

If the thermoelectric bridge of CeB_6 possesses a Seebeck coefficient of S = 150 μV/K, which corresponds to the average value reported in the literature, then as can be seen in the Table 2 and Table 3, the resulting voltage can reach microvolts.

The obtained characteristics are encouraging, they ensure the competitiveness of the thermoelectric detector with the superconducting single-photon detectors described in the literature. The simplicity of the thermoelectric sensor design, the lack of stringent requirements for maintaining the operating temperature and the relatively high operating temperature (twice higher than the boiling point of liquid helium) are additional advantages of the

thermoelectric detectors based on CeB_6.

The results included in this work were presented earlier, particularly in the conferences "Nano 2014" and "TechConnect World Innovation 2015" [13-14].

Acknowledgements

The authors wish to thank A.M. Gulian for fruitful discussions. This work was supported by the RA MES State Committee of Science and Russian Foundation for Basic Research (RF) in the frames of the joint research projects SCS 15RF-018 and RFBR 15-53-05047 accordingly.

References

[1]. R. H. Hadfield, Single-photon detectors for optical quantum information applications, *Nature Photonics*, Vol. 3, No. 12, December 2009, pp. 696-705.

[2]. K. D. Irwin, Seeing with Superconductors, *Scientific American*, Vol. 295, No. 5, November 2006, pp. 86-94.

[3]. T. Yamashita, S. Miki, H. Terai, Z. Wang, Low-filling-factor superconducting single photon detector with high system detection efficiency, *Optics Express* Vol. 21, No. 22, 2013, pp. 27177-27184.

[4]. A. Gulian, K. Wood, D. van Vechten, G. Fritz, Cryogenic thermoelectric (QVD) detectors: Emerging technique for fast single-photon counting and non-dispersive energy characterization, *Journal of Modern Optics*, Vol. 51, No. 9-10, 2004, pp. 1467-1490.

[5]. A. A. Kuzanyan, A. S. Kuzanyan, Thermoelectric nanowire single-photon detector, *Proceedings of SPIE,* Vol. 8773, 2013, 87730L.

[6]. V. A. Petrosyan, Hexaborides of rare earths as a sensor material for thermoelectric single-photon detectors, *Journal of Contemporary Physics*, Vol. 46, No. 3, 2011, pp. 125-129.

[7]. A. A. Kuzanyan, Nanosensor for thermoelectric single-photon detector, *NanoStudies*, Vol. 9, 2014, pp. 93-102.

[8]. T. R. Waite, R. S. Craig, W. E. Wallace, Heat Capacity of Tungsten between 4 and 15° K, *Physical Review*, Vol. 104, No. 5, 1956, pp. 1240-1241.

[9]. Efunda Web Portal (http://www.efunda.com/materials/elements/TC_Table.cfm?Elment_ID=W).

[10]. S. R. Harutyunyan, V. H. Vardanyan, A. S. Kuzanyan, V. R. Nikoghosyan, S. Kunii, K. S. Wood, A. M. Gulian, Thermoelectric cooling at cryogenic temperatures, *Applied Physics Letters*, Vol. 83, Issue 11, 2003, pp. 2142-2144.

[11]. Y. Peysson, C. Ayache, B. Salce, J. Rossat–Mignod, S. Kunii, T. Kasuya, Thermal properties of CeB_6 and LaB_6, *Journal of Magnetism and Magnetic Materials*, Vol. 59, 1986, pp. 33-40.

[12]. A. A. Kuzanyan, V. A. Petrosyan, A. S. Kuzanyan, Thermoelectric single-photon detector, *Journal of Physics: Conference Series*, Vol. 350, 2012, 012028.

[13]. A. A. Kuzanyan, A. S. Kuzanyan, Nanosensor for thermoelectric single-photon detector, *Abstracts of the 3rd International Conference "Nanotechnologies" (Nano – 2014)*, Tbilisi, Georgia, 20-24 October, 2014, pp. 72.

[14]. A. S. Kuzanyan V. R. Nikoghosyan, A. A. Kuzanyan, Simulation of Photon Thermalization in a Single-Photon Detector on The Basis of CeB_6 Thermoelectric Sensor, *Program of the TechConnect World Innovation, Conference & Expo*, Washington DC, USA, 14-17 June 2015, W6.409, p. 104. http://www.techconnectworld.com/World2015/a.html?i=1091